Accepted Manuscript

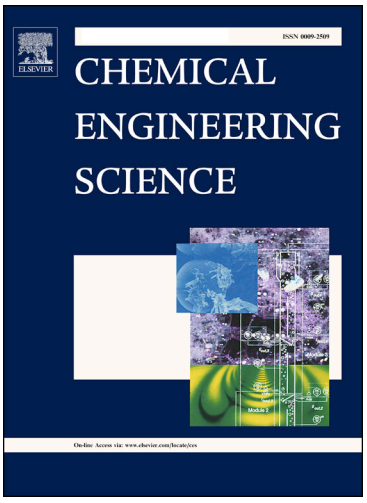

Particle motion and heat transfer in an upward-flowing dense particle suspension: application in solar receivers

P. García-Triñanes, J.P.K. Seville, R. Ansart, H. Benoit, Leadbeater T.W., Parker D.J.

PII: S0009-2509(17)30720-0
DOI: https://doi.org/10.1016/j.ces.2017.11.041
Reference: CES 13927

To appear in: *Chemical Engineering Science*

Received Date: 19 July 2017
Revised Date: 31 October 2017
Accepted Date: 25 November 2017

Please cite this article as: P. García-Triñanes, J.P.K. Seville, R. Ansart, H. Benoit, L. T.W., P. D.J., Particle motion and heat transfer in an upward-flowing dense particle suspension: application in solar receivers, *Chemical Engineering Science* (2017), doi: https://doi.org/10.1016/j.ces.2017.11.041

Particle motion and heat transfer in an upward-flowing dense particle suspension: application in solar receivers

García-Triñanes P. [1,*], Seville J.P.K. [1], Ansart R.[2], Benoit H.[3], Leadbeater T.W. [4], Parker D.J. [4]

[1] Chemical and Process Engineering, Faculty of Engineering and Physical Sciences, University of Surrey, Guildford, GU2 7XH, United Kingdom

[2] Université de Toulouse; INPT, UPS; Laboratoire de Génie Chimique ; 4, Allée Emile Monso, F-31030 Toulouse, France

[3] PROMES-CNRS, Materials and Solar Energy Laboratory, Font Romeu, 66120, France

[4] Positron Imaging Centre, School of Physics and Astronomy, University of Birmingham, Edgbaston, Birmingham, B15 2TT United Kingdom

Abstract:

Concentrated solar power (CSP) plants conventionally make use of molten salt as the heat transfer medium, which transfers heat between the solar receiver and a steam turbine power circuit. A new approach uses particles of a heat-resistant particulate medium in the form of many dense upward-moving fluidised beds contained within an array of vertical tubes within the solar receiver. In most dense gas-solid fluidisation systems, particle circulation is induced by bubble motion and is the primary cause of particle convective heat transfer, which is the major contributing mechanism to overall heat transfer. The current work describes experiments designed to investigate the relationship between this solids convection and the heat transfer coefficient between the bed and the tube wall, which is shown to depend on the local particle concentration and their rate of renewal at the wall. Experiments were performed using 65 µm silicon carbide particles in a tube of diameter 30mm, replicating the conditions used in the real application. Solids motion and time-averaged solids concentration were measured using Positron Emission Particle Tracking (PEPT) and local heat transfer coefficients measured using small probes which employ electrical resistance heating and thermocouple temperature measurement. Results show that, as for other types of bubbling beds, the heat transfer coefficient first increases as the gas flow rate increases (because the rate of particle renewal at the wall increases), before passing through a maximum and decreasing again as the reducing local solids concentration at the wall becomes the dominant effect. Measured heat transfer coefficients are compared with theoretical approaches by Mickley and Fairbanks packet model and Thring correlation. The close correspondence between heat transfer coefficient and solids movement is here demonstrated by PEPT for the first time in a dense upward-moving fluidised bed.

Keywords:

*Correspondence concerning this article should be addressed to : P.GarciaTrinanes@gre.ac.uk

Preprint submitted to CES: 20th July 2017
Reviewed 31st October 2017

Solar energy; fluidisation, dense particle suspension, heat transfer, wall region contact time

GRAPHICAL ABSTRACT

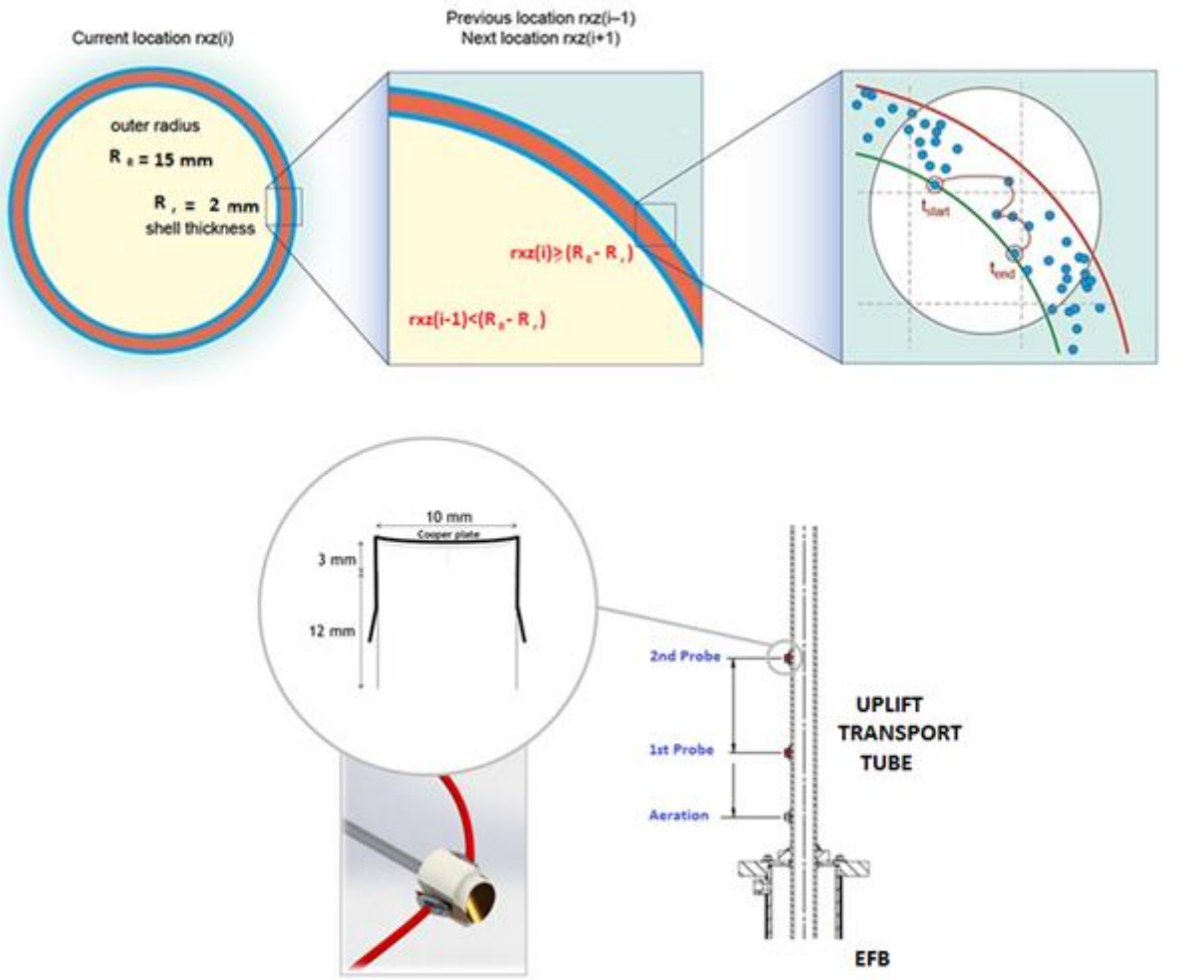

Preprint submitted to CES: 20th July 2017
Reviewed 31st October 2017

Notation

PEPT	Positron Emission Particle Tracking
DPS	Dense particle suspension
CSP	Concentrated solar power
HTF	Heat transfer fluid
DiFB	Dispenser Fluidised Bed
k_e^o	Effective radial thermal conductivity, W/m·K
C_p	Solid heat capacity, J/kg·K
U_{mf}	Minimum fluidising velocity, m/s
U_{mb}	Minimum bubbling velocity, m/s
ε_{mf}	Minimum fluidisation velocity associated void fraction, m/s
ρ_p	Particle density, kg/m^3
U_{ae}	Aeration velocity, m/s
U_o	Optimum fluidising velocity, m/s
h	Heat-transfer coefficient, W/m^2·K
d_p	Particle size, 10^{-6} m
q	Power supplied to the heater, W
S_{pr}	Surface area of the probe, m^2
R_{pr}	Resistance of the probe, Ω
I	Electrical current, A
T_b	Dense phase suspension temperature, ˚C
T_s	Surface temperature of the heater, ˚C
R_R	Uplift transport tube radius, 10^{-3} m
R_r	Shell thickness, 10^{-3} m
$r_{xz}(i)$	Current tracer location
$r_{xz}(i-1)$	Previous tracer location
$r_{xz}(i+1)$	Next tracer location
τ	Wall contact time, s
φ	wall region, 10^{-3} m
t_r	Residence time of the emulsion packet at the heat transfer surface, s

Preprint submitted to CES: 20th July 2017
Reviewed 31st October 2017

1. INTRODUCTION

Concentrated Solar Power (CSP) plants have received recent attention as an alternative to photovoltaics. In CSP, solar radiation is focused using diverse mirror or lens configurations onto a **solar receiver** where it raises the temperature of a **heat transfer fluid** (HTF), which is in turn used to generate steam that powers a turbine-generator to produce electricity[1] *(Flamant et al.,2013).*

The classical **heat transfer and thermal storage fluids** are synthetic **oils and molten salts**. Oils have limitations since they are stable only up to 400 °C and present significant safety issues due to their flammability. Although the use of **molten salts** improves performance it is far from optimal since they are restricted to operating temperatures below 550 °C and they suffer from corrosion problems at high temperatures which significantly increases maintenance costs. In addition molten-salt systems are affected by freezing problems if the salt temperature drops too low, and therefore require high parasitic power consumption to prevent this.

Liquid metals present potential alternative heat transfer media, since some are relatively stable at high temperatures and typically offer good thermal properties. Their use is limited by inherent **safety risks**, since they will combust in contact with air and their large hydration energy results in a vigorous exothermic reaction with water. Moreover, liquid metals interact with structural materials at high temperature[2]. *(Pacio and Wetzel, 2013).*

The purpose of this research is to evaluate a further alternative: the use of **small particles suspended in gas in the form** of a **dense upward-flowing fluidised bed**. The stirring effect induced by the gas bubbles within the bed results in relatively uniform axial and radial temperature distribution in the dense phase and good heat transfer from the walls.

The term **dense suspension** here means an overall phase concentration of particles comparable to that encountered in conventional fluidised beds (≥ 25%). **Dense particle suspensions** offer the possibility of operation at elevated temperatures which is fundamental for achieving higher **heat transfer rates** which are essential in order to achieve economically attractive plant designs. Operation is favoured if the solid particles selected have a large **thermal conductivity** and high **heat capacity,** which would enable the additional benefit of **thermal storage**.

Preprint submitted to CES: 20th July 2017
Reviewed 31st October 2017

Similarly, operational aspects such as safety and corrosion risk are minimised and the power consumption for pumping is small compared with the alternatives.

Fluidisation offers excellent **heat transfer** between the particles and the wall, because the **particle motion** within the bed ensures that there is frequent **renewal at the wall** surface. **Heat transfer in fluidised beds** occurs by conduction, convection (of both gas and solids) and radiation, with **convection** dominating except at elevated temperatures. Especially for **small particles**, **gas convection** hardly contributes in comparison with the **solid convection**, which is the subject of the study reported here.

Heat transfer by convection of solids depends on the **local solids concentration** and **the rate at which particles are replaced at the wall.** An increase in **gas velocity** affects these two parameters in different ways: as **gas velocity** is increased, the particle renewal frequency at the wall is higher, so that the **heat transfer coefficient** increases**.** Beyond a certain point, however, further increase in the gas flow can cause the local solids density to decrease and the surface to become blanketed by excess gas, so causing a reduction in heat transfer coefficient.

Many predictive models for heat transfer in fluidised beds are available[3] *(Botterill, 1975),* notably the so-called **packet model** of *Mickley and Fairbanks*[4] *(Mickley and Fairbanks*, 1955), which considers heat transfer to occur by the motion of **clusters of particles** called "packets", with characteristic void fraction and thermal conductivity. Packet motion is driven by the gas and packets periodically make contact with the heat transfer surface and remain there for a **characteristic residence time** exchanging heat with the surface, before being swept away and replaced by a new packet.

The motion of the packets is directly related to the flow of gas bubbles through the bed, and their surface scouring action will increase as bubble flow increases, up to a point where the surface becomes blanketed by bubbles, as indicated earlier.

According to this approach, the instantaneous heat transfer coefficient can be obtained as follows:

$$h_{packet} = \frac{2}{\sqrt{\pi}}\sqrt{\frac{k_e^o \rho_p (1-\varepsilon_{mf}) C_p}{\tau}} \qquad \{1\}$$

where k_e^o represents the thermal conductivity of the medium, ρ_p is the particle density, ε_{mf} is the void fraction at minimum fluidisation, C_p the heat capacity of the solid particles and τ the "packet replacement time". As indicated above, increased gas velocity decreases τ, so increasing the heat transfer coefficient.

The Mickley and Fairbanks packet theory was modified by *Baskakov*[5] *(Baskakov, 1964)* who proposed a time-independent additional resistance near the wall caused by a differential void fraction between the emulsion and the surface region. He suggested that the thickness of this film is proportional to the particle size.

Thring[6] *(Thring, 1977)* also suggested that during the residence time the emulsion packet is separated from the heat-transfer surface by a gas gap. He pointed out some of the drawbacks of previous models such as the fact that the emulsion packets cannot reasonably be considered to have uniform thermal properties, since the entire temperature gradient turns out to occur in a distance from the heat-transfer surface equivalent to a few particle diameters.

Ozkaynak and Chen[7] *(Ozkaynak and Chen, 1980)* confirmed the validity of the packet model for small particles with different physical and thermal properties. In their study they used the difference of dielectric constants between gas and solids to obtain real-time measurements of fluctuating particle concentration at surfaces immersed in fluidised beds. According to their results the heat transfer coefficient decreases with increasing particle size.

The first attempt to interpret fluidised bed heat-transfer results using single-particle trajectories obtained from Positron Emission Particle Tracking (PEPT) was made by *Wong and Seville*[8] *(Wong and Seville, 2006).* PEPT is ideally suited to this task since it enables a single particle of the bed material to be tracked at speeds up to the maximum experienced in this application, to a precision of ± about 1mm, within a bed of opaque material and within a retaining tube with metal walls. A review of the capabilities of the technique is given by *Seville et al*[9]*. (Seville et al, 2009).*

Wong and Seville[8] *(Wong and Seville, 2006)* studied particle motion around horizontal immersed tubes in a conventional bubbling fluidised bed typical of, for example, a combustor. They demonstrated the variation of residence time and local solids concentration with angular position around the tube and showed how this leads to the observed angular variation in heat transfer coefficient.

The current work includes similar measurements but at the wall of the bed in a quite different flow regime: dense upward flow in a narrow tube of high height-to-diameter aspect ratio.

2. MATERIALS AND METHODS

The work described here concerns particle motion in a single uplift transport tube (1.1 m in length and 30 mm in diameter), which is selected to be representative of the array of tubes in a full-scale solar receiver[10] *(Perez-Lopez, 2016),* but operates at ambient temperature. The single transport tube is operated in a continuous loop, such that particles flow upward in the transport tube, are disengaged from the gas and then travel downward under gravity to be reintroduced to the base of the apparatus.

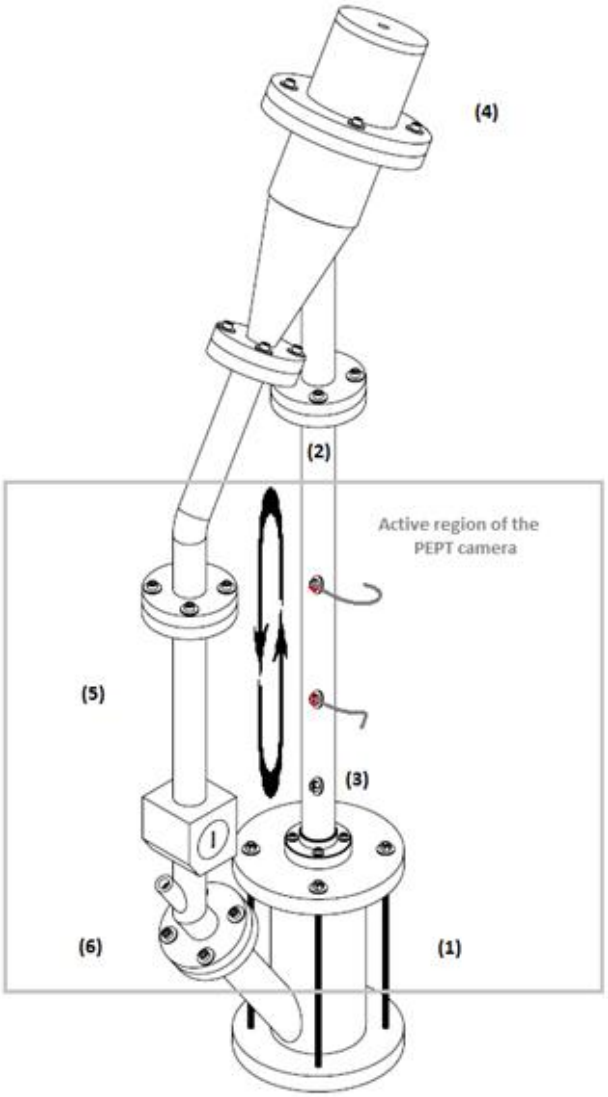

Figure 1. Schematic diagram of the experimental set-up.

The full apparatus (Fig. 1) consists of a pressurised bubbling fluidised dispenser bed (DiFB) (1), with a sintered brass distributor, into which the transport tube is partially submerged. The dense suspension rises up the transport tube (2), which has additional aeration –all gas through one nozzle- (3) and terminates in a cyclone-like disengaging zone (4). From here the disengaged solids fall under gravity into a downcomer (5). The solids are 65 µm SiC particles (ρ_p=3210 kg/m3) and the total charge is 1.7kg.

It is necessary to feed particles from the downcomer into the pressurised dispenser bed in a controlled way. For this purpose a bespoke inclined eductor was designed (6). The apparatus is also equipped with a pressure control

system and a data logger connected to a Labview interface in order to obtain pressure readings using pressure transducers at different points in the uplift transport tube. Further details can be found elsewhere[11] (*Garcia-Triñanes et al., 2016).*

The minimum fluidization velocity was measured in a column of 200 mm by using the Davidson and Harrison method (Umf= 0.005 m/s; Umb=0.008 m/s). [J.F. Davidson, D. Harrison, Fluidized Particles, Cambridge University Press, 1963]) The SiC particles were fluidised with compressed air in the 90 mm diameter DiFB at a constant fluidisation flow rate of 0.096 m/s. The pressure created in this dispenser bed pushes the particles up into the fluidised transport tube.

In order to maintain good fluidisation in the transport tube, it was found necessary to provide additional aeration to the uplift transport tube[12] *(*Boissière *et al 2015).* The aeration rate has therefore been found to be the single most important influence on behaviour in the transport tube. In order to investigate the influence of the aeration flow rate (U_{ae}), heat transfer tests at four different aeration velocities were carried out: U_{ae}/U_{mb}= 2.5, 5, 7.5 and ultimately 10 m/s using a fluidisation velocity (U_f) of 0.096 m/s.

PEPT data were used to determine the trajectories of a single particle tracer inserted in the bed when operating under different aeration velocities. For each aeration gas velocity, data were acquired with the system operated for a total of 2 hours. The location of the tracer covered a total height of 500 mm of the transport tube; this is less than the full height since accurate tracking is not possible near the edges of the field of view of the camera. These data were further analysed, yielding residence times close to the wall, occupancy (the proportion of the total run time which the tracer spends in each volume element), solids mass flux and lateral solids mixing and dispersion for each of the operating conditions.

Heat transfer measurements were carried out using two copper platen heat transfer probes (10 mm in diameter), which were specially designed for this purpose and are shown schematically in Figure 2. The first heat transfer probe is located above the aeration port and the second one further up in the transport tube separated by 200 mm.

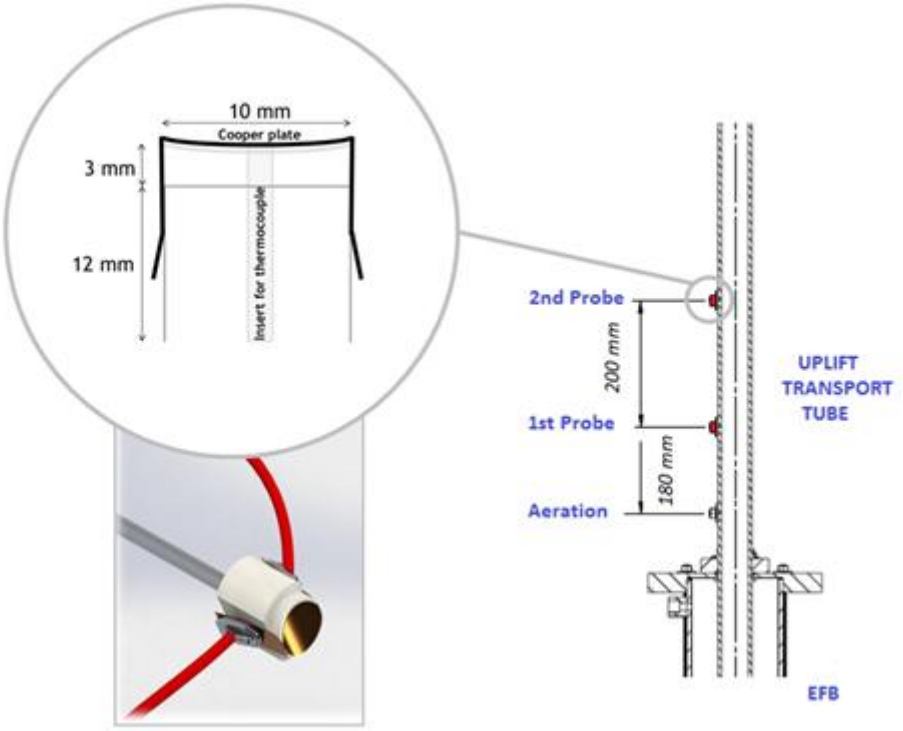

Figure 2. Aspect and location of the heat transfer probes mounted to the uplift transport tube.

The operating principle of the measurement is that of measuring the electrical energy required to keep the probe at a given temperature above that of the bed ($\approx 55\ ^{\circ}C$). This gives the heat transferred from the probe. Taking into account the heat transfer area and the temperature difference between the probe and the bulk of the particles, the wall-to-bed heat transfer coefficient, h, can then be obtained:

$$\boldsymbol{h = \frac{q}{S_{pr}(T_s - T_b)}} \qquad \{2\}$$

where q is the power supplied to the heater, I^2R_{pr} (W), S_{pr} is the surface area of the heater ($7.85 \cdot 10^{-5}$ m^2), T_s is the surface temperature of the heater (˚C), measured by attaching a Type K thermocouple to its surface, T_b is the dense phase suspension temperature (˚C) obtained with a second thermocouple. Both T_s temperatures are compared with a set point temperature. Calibrations were carried out to both voltmeter and ammeter.

As indicated above, probes were located at two positions and were operated independently. The heat transfer surface was of copper, due to its good thermal conductivity, and each probe was inserted at with the wall of the transport tube so as to attenuate interference with the upward flow of the suspension (lateral heat losses are considered negligible). Further details of this type of probe design are given by *Ganzha and Saxena*[13]. *(Ganzha and Saxena, 1998)*

3. RESULTS AND DISCUSSION

3. 1. Analysis of particle motion

A typical solids streamline pattern in the transport tube is presented in Fig. 3 derived from particle trajectory data and the local instantaneous particle velocities as calculated from the 6-point method *(Ansart, 2017).* Note that the colorbar corresponds to average total velocity. This figure shows the motion of the tracer and recirculation near the wall.

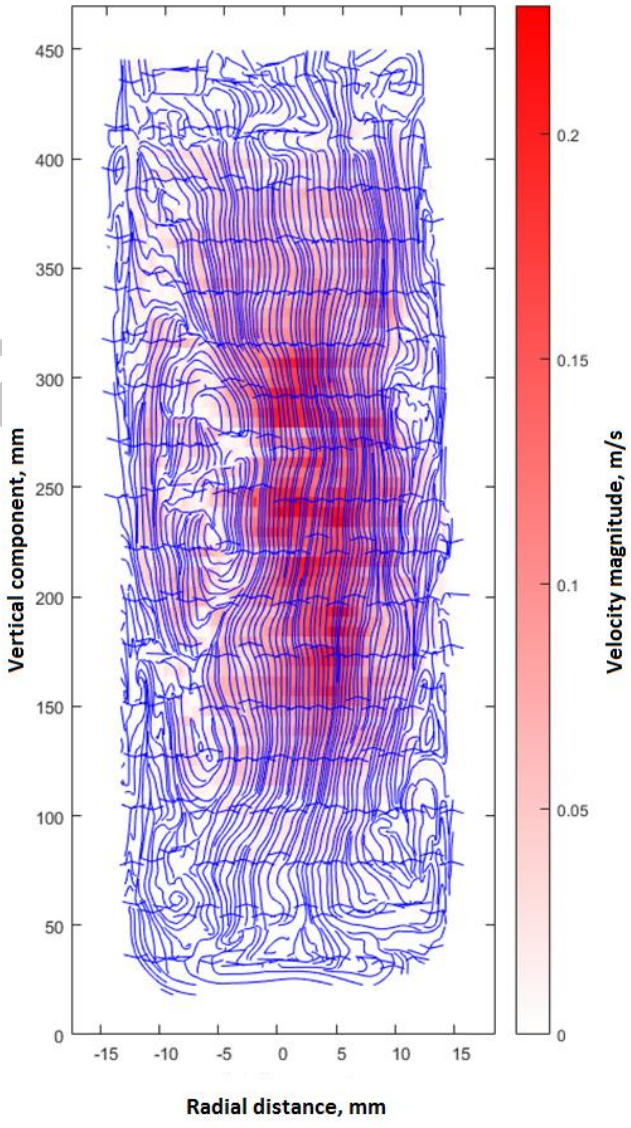

Figure 3. Instantaneous solids streamline pattern in the transport tube (U_{ae}/U_{mb}=5).

Figure 4 shows a typical example of a particle trajectory in the transport tube. As in conventional fluidised beds, motion is generally upward in the centre as particles are caught in the wake of bubbles[15] *(Stein, 2000).* Particles are periodically shed from their associated bubbles; they may then become reattached to a new bubble or remain in the generally down-flowing region near the wall[16] *(Garcia-Trinanes, 2016).* The figure shows examples of both these behaviours.

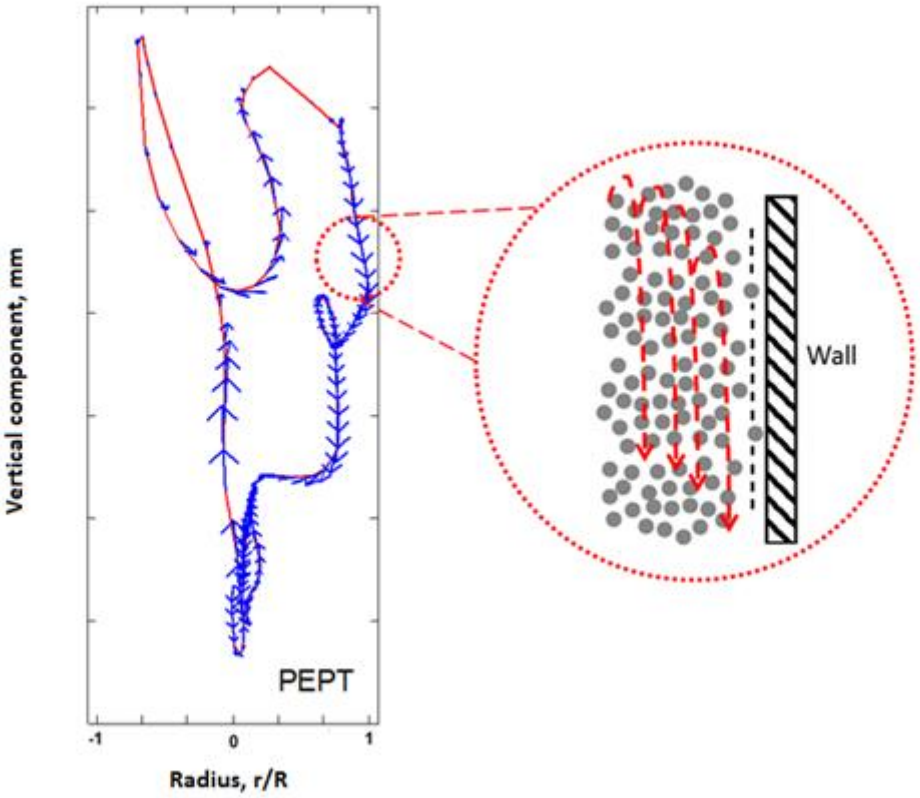

Figure 4. Schematic representation of the stream of particles mechanism for an upward dense particle suspension.

3.2. Residence time at the wall and its relationship to heat transfer

From the PEPT data it is possible to determine the position of the tracer particle at every stage of its movement. However, there is an inherent uncertainty in position, due to the PEPT location method[9] (Seville, 2009), which is ≈ 0.5 mm in this case. It is therefore not possible to determine unambiguously that the tracer has made contact with a given surface. An approach which can be followed, as in previous work by *Wong and Seville*[8] *(Wong and Seville, 2006),* is to define virtual surfaces which are concentric with the surface of interest but at a certain

distance from it, and to measure the residence time of the tracer within each surface, i.e. within a "wall region" of a certain thickness. Wall regions of different thicknesses were investigated, with 2 mm chosen for the bulk of the measurements reported here.

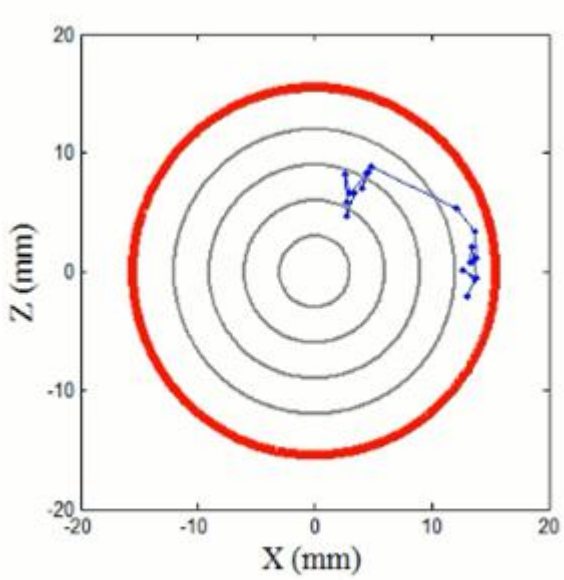

Figure 5. Example of trajectory in the plan view showing the tracer approaching and leaving the wall (time-duration 150 ms).

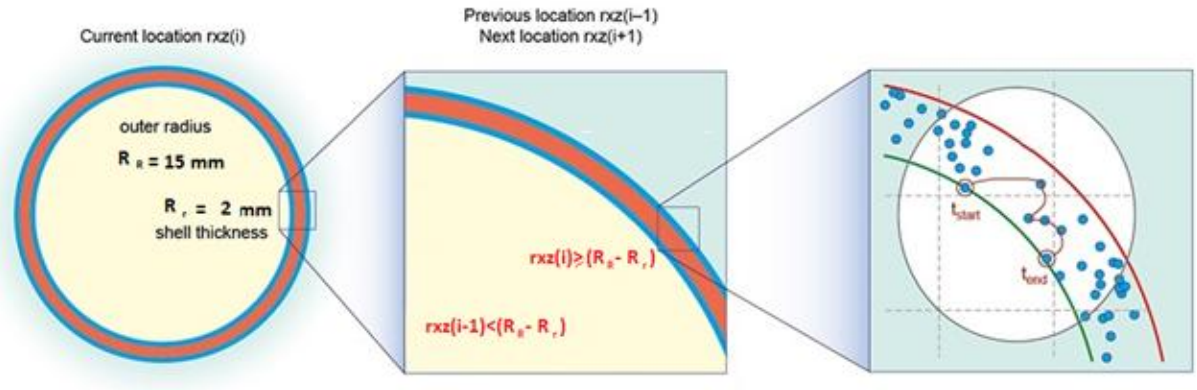

Figure 6. Principle of determining the time in the wall region.

(For interpretation of the references to color, the reader is referred to the web version of this article.)

Figure 5 shows the trajectory of a particle approaching the wall and Fig 6 shows the principle of the measurement of residence time in the wall region. Locations within the wall region be determined, from which a duration of the trajectory within the region of interest can be obtained. Under the conditions of these experiments, the residence time in the wall region can be determined to within 10 ms. During this PEPT experiment, the tracking precision of a 68 microns tracer reaches 0.85 mm in 3D with a location frequency of 10 Hz for a tracer moving at 0.2 m/s.

(Ansart, 2017).

It may be noted that the time frequency of location using PEPT is approximately, but not completely, constant. The reason for this is that the PEPT algorithm uses a fixed number of events (pairs) for each location. The frequency of such events depends on position of the tracer in the camera.

Count rates are higher with the tracer located in the centre rather than at the edges of the field of view. There will also be effects of the amount of material to be penetrated (attenuation) and time (tracer decaying). Finally, the algorithm eliminates about 80% of the collected events, converging on the most likely location, and bases the time stamp on the average of the remaining events.

Figure 7 shows locations in a 2 mm shell at a height between 100-250 mm above the aeration port during a typical PEPT experiment, and the corresponding histogram of locations per visit in the wall region is shown:

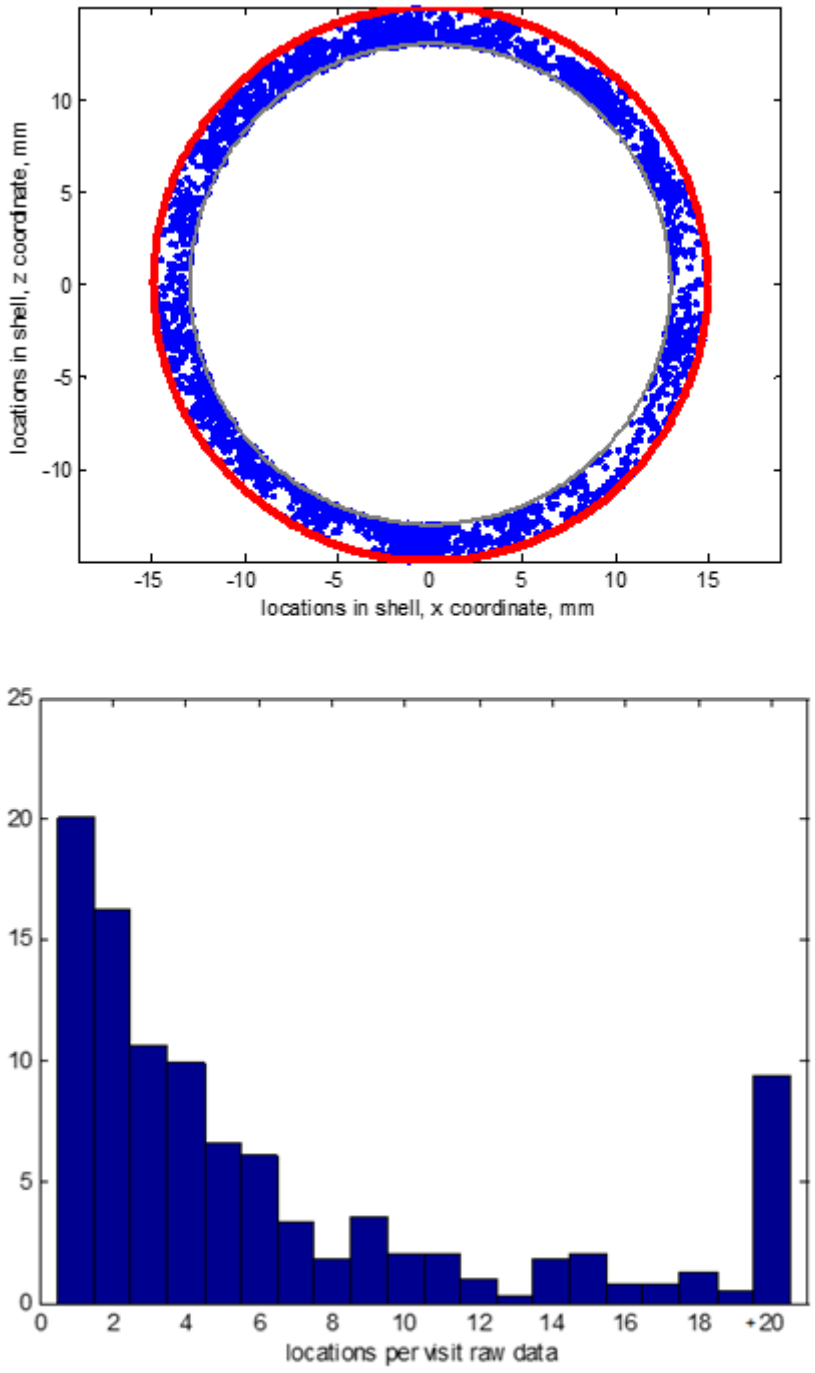

Figure 7. Locations in a 2 mm shell (top) and percentage of locations per visit (bottom); 2 hours of data acquisition.

Given the inherent positional uncertainty, one location within the wall region is insufficient to determine that the tracer has visited the region; 2 or more locations give higher probability that it has done so. Similarly, longer residence times are equivalent to more locations within the wall region, giving both a higher probability that they correspond to real visits and a more accurate measurement of the residence time itself. Residence times below 20 ms are invalid as they correspond to a single location within the wall region.

Following previous studies[7, 17] *(Ziegler, 1964)* and *(Ozkanak and Chen, 1980)* the distribution of residence times in the wall region was found to be approximately log-normal, as shown in Fig 8, again for the region of the transport tube between 100-250 mm above the aeration port.

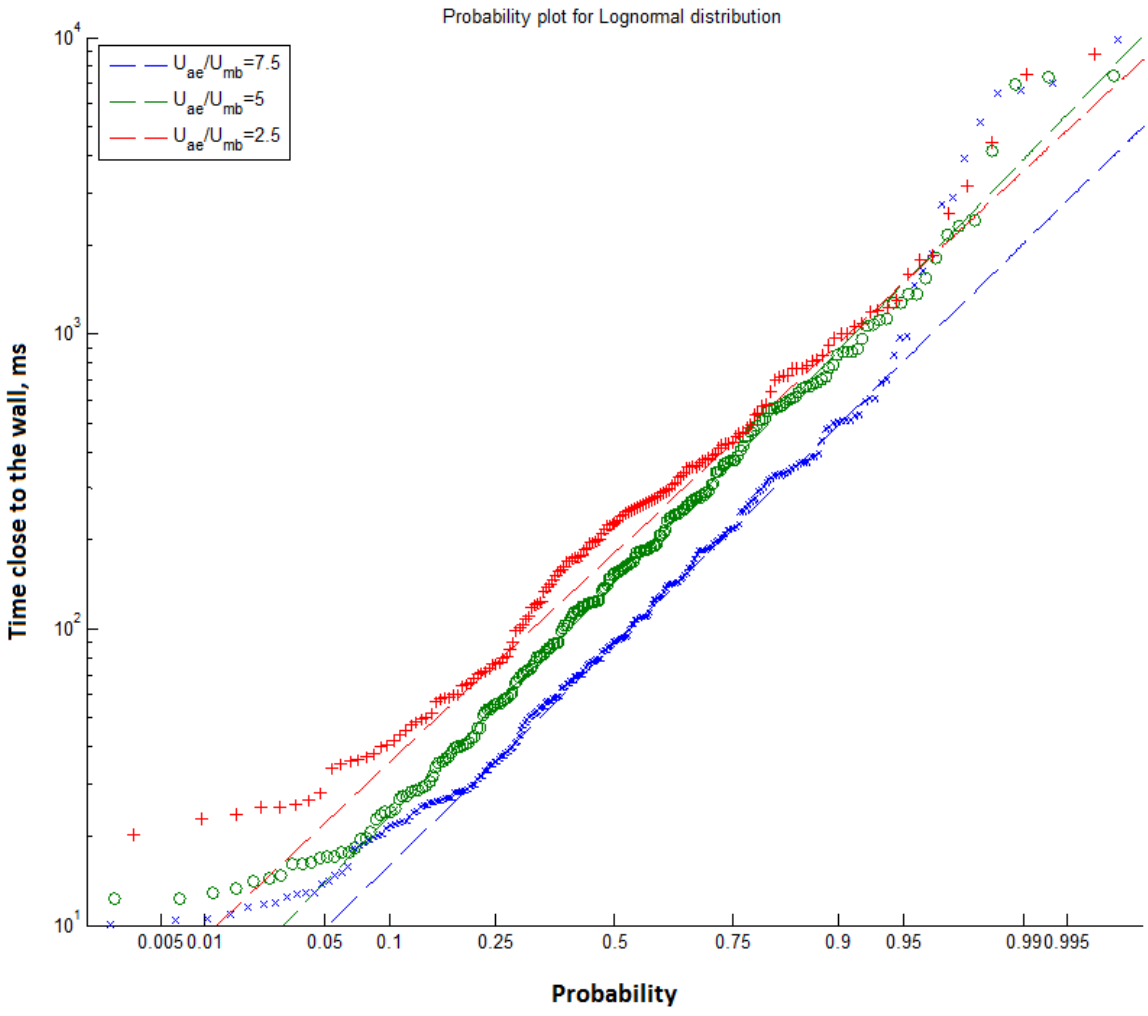

Figure 8. Distribution of residence times in the wall region, for three values of U_{ae}/U_{mb} (wall region φ=2 mm)

These results are consistent with observations that aeration velocity increases bubble frequency, so that particles residing on the wall surface are more frequently displaced.

Fig. 9 shows the average contact time (τ) in the wall region (using PEPT data) for the section of the transport tube between 100-250 mm above the aeration port as a function of the radial distance to the wall. An increase of the aeration decreases the residence time of the particle close to the wall.

Two different regions, can be clearly identified: If the tracer goes straight to the wall, assuming some average velocity, the residence time is proportional to the width of the annulus from the wall. If it takes a meandering path and goes everywhere then the residence time depends on the volume of the annulus, since height is constant.

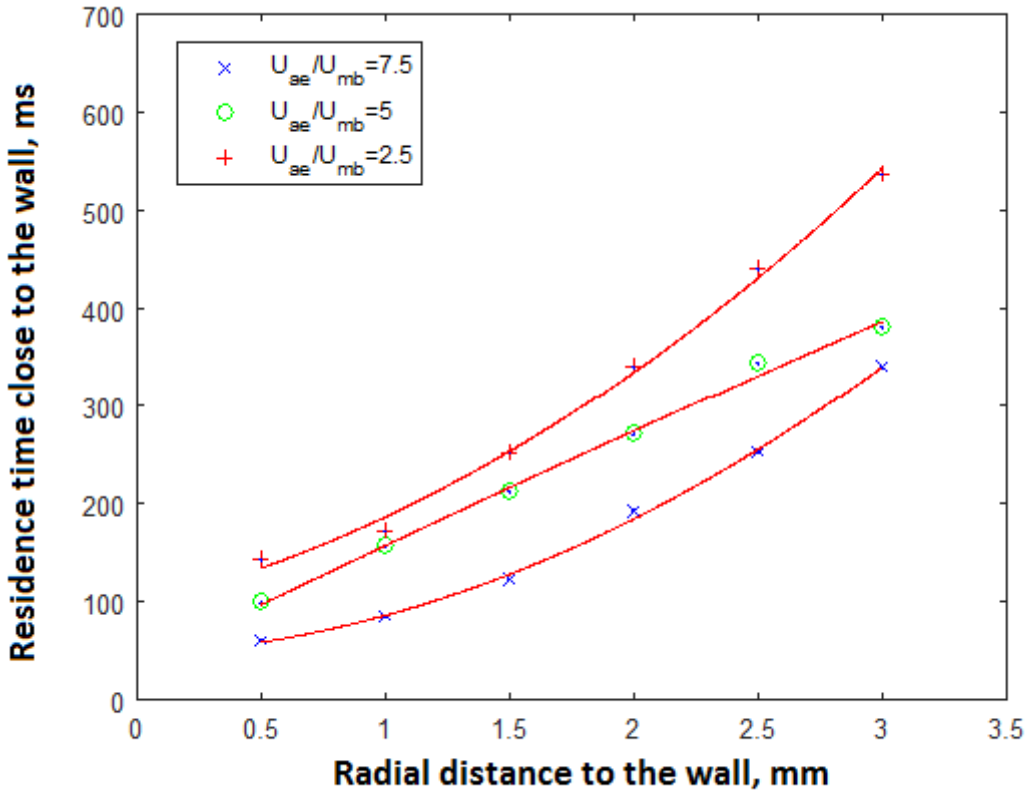

Figure 9. Variation in residence time with decreasing radial distance to the wall.

Table 1 shows relationship between experimental values of residence time (τ) and radial distance to the wall (φ). For each of the operating conditions tested, a second order polynomial is fitted directly to the raw data of the trial.

Table 1. Variation in residence time with radial distance to the wall.

Operating conditions	*Mathematical expression*	*R^2 (determination coefficient)*
U_{ae}/U_{mb}=7.5	$\tau = 29.044\varphi^2 + 11.224\varphi + 45.622$	0.9981
U_{ae}/U_{mb}=5	$\tau = -2.1214\varphi^2 + 123.52\varphi + 35.67$	0.9957
U_{ae}/U_{mb}=2.5	$\tau = 29.729\varphi^2 + 59.641\varphi + 96.881$	0.9965

Fig.10 presents a comparison between the sample median of the residence time in the wall region ($\varphi = 2\,mm$) in the region of the tube between 100-250 mm above the aeration port and the prediction suggested by Thring[6] (Eq. 3) *(Thring, 1977)* for the residence time of the emulsion packet at the heat transfer surface, showing satisfactory agreement with the predictions of this correlation that depends on minimum (U_{mf}) and optimum (U_o) fluidising velocity and particle size (d_p).

$$t_r = 8.932\left[\frac{d_p g}{U_{mf}^2\left(\frac{U_o}{U_{mf}} - 1\right)^2}\right]^{0.0756}\left(\frac{d_p}{2.54}\right)^{0.5} \qquad \{3\}$$

The increasing departure from the Thring correlation at the highest aeration velocity may be connected with slugging rather than bubbling behaviour[18] (Kong, 2017).

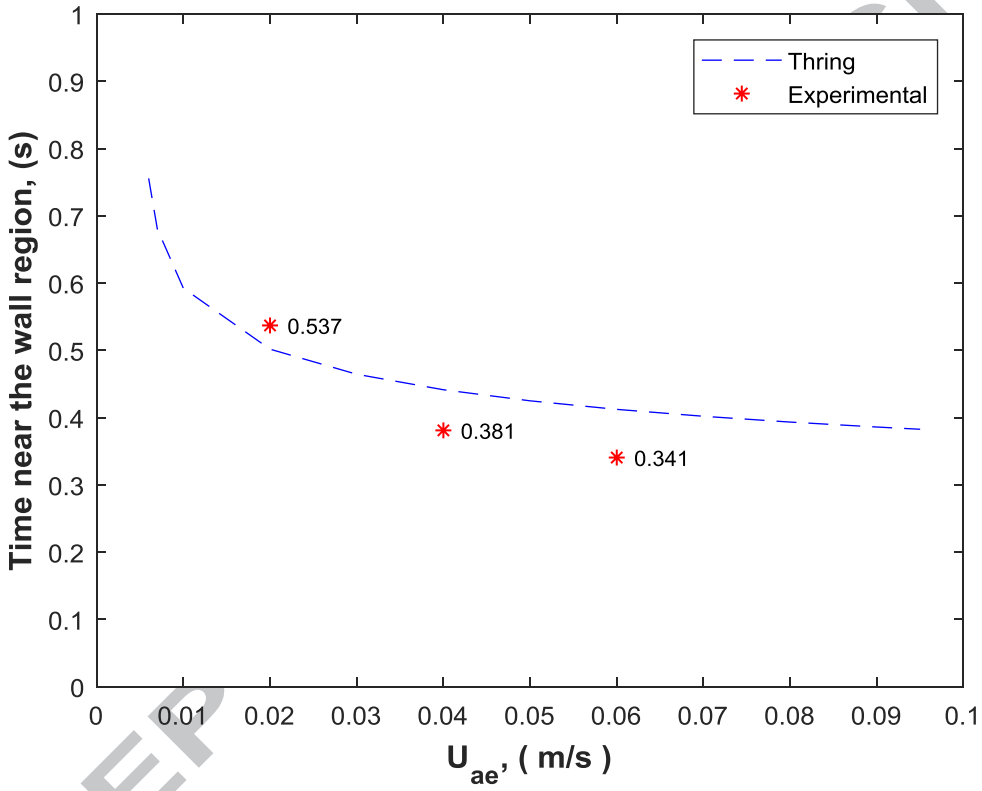

Figure 10. Estimation of the time in the wall region as a function of the aeration velocity using Thring (Eq.3).

3.3 Heat transfer coefficient

As shown earlier, wall probes enabled the heat transfer coefficient to be determined simultaneously with the PEPT measurements. Figure 11 illustrates the variation in heat transfer coefficient as a function of the aeration gas velocity (U_{ae}/U_{mb}).

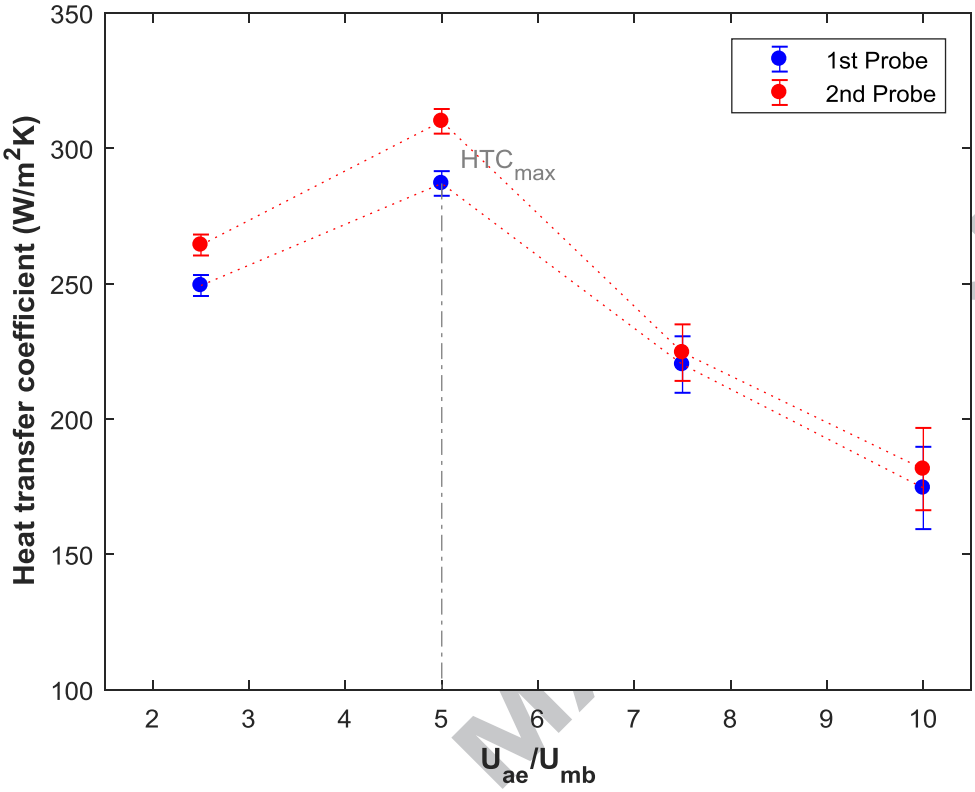

Figure 11. Measurement of the bed-to-surface heat transfer coefficient as a function of the aeration gas injection flow rate.

Figure 12 shows the effect of aeration flow rate on solids volume fraction and residence time in the wall region. These competing effects cause a maximum in the heat transfer coefficient, as shown in Fig. 11.

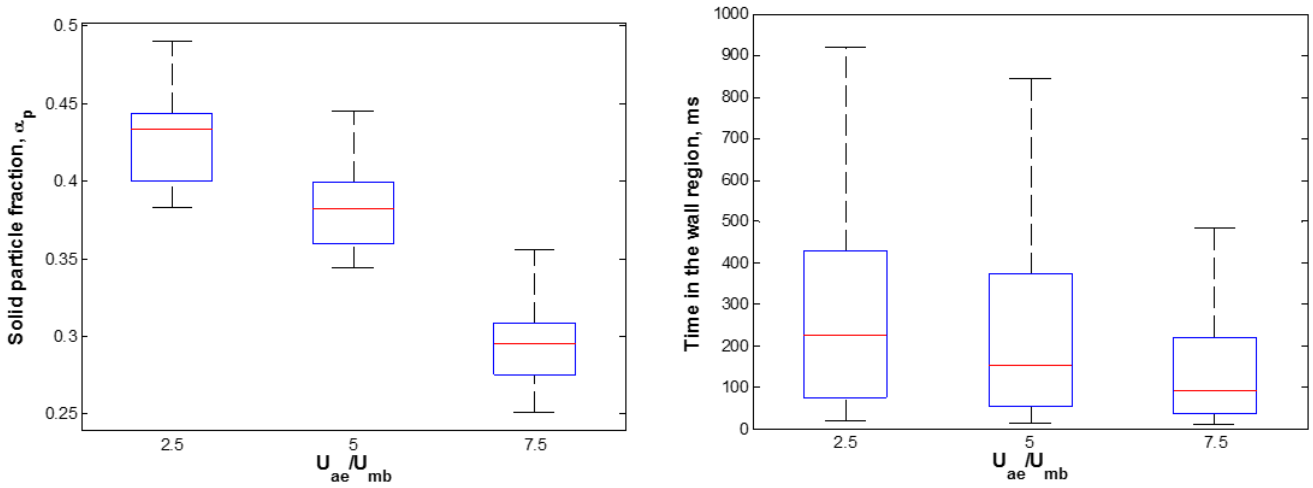

Figure 12. Effect of the aeration on the solids volume fraction and on the residence time of the particles in the wall region.

Figure 13 shows a comparison of the measured heat transfer coefficients with the predictions of the packet model, using residence/contact times measured using PEPT, and the correlation for the maximum obtainable heat transfer coefficient from *Zabrodsky*[19] *(Zabrodsky, 1966),* and showing fair agreement. The measured heat transfer coefficient at the highest gas velocity/shortest residence time is well below the packet model predictions, presumably because blanketing of the heat transfer surface reduces heat transfer under these conditions. This is not accounted for in the Mickley and Fairbanks model.

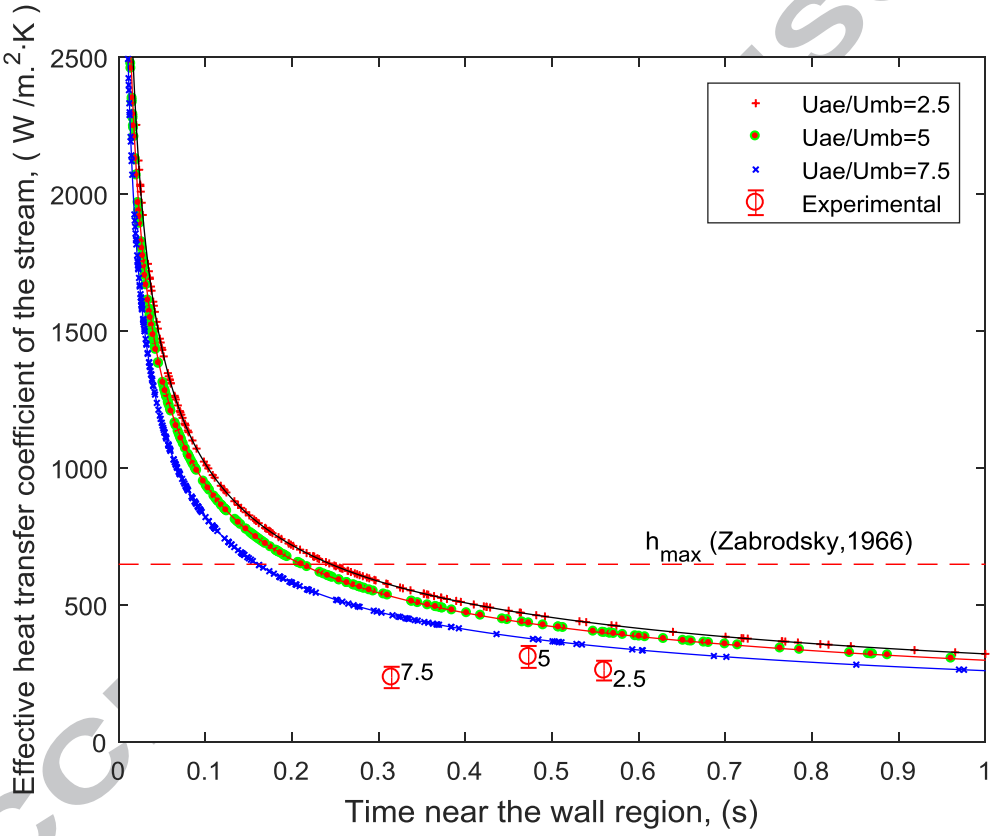

Figure 13. Heat transfer coefficient of the stream as a function of the time in the wall region using the Mickley and Fairbanks packet model and experimental results calculated using the heat transfer probe.

4. Conclusions

Particle trajectories have been measured and associated wall-to-bed heat transfer coefficients determined for dense fluidised suspensions of particles of silicon carbide (65 microns) moving upward in a small diameter tube (30 mm) at different aeration velocities from 0.02 to 0.06 m/s.

As in other types of bubbling fluidised bed, the local concentration of particles and their movement at the wall play a decisive role in the heat transfer, and the operating parameters influence the heat transfer through their effect on particle concentration and movement.

Heat transfer coefficients in the range 180-320 W/m^2K were measured, rising to a maximum as the aeration velocity increases and then falling as the heat transfer surfaces become blanketed by gas.

Particle residence times at the wall were measured and found to be approximately distributed according to a log-normal distribution, as previously suggested by *Ozkanak and Chen (1980).* Median residence times varied from 100 to 250ms in the parameter range studied.

Experimentally-obtained heat transfer coefficients were found to be in fair agreement with predictions of the correlations by *Thring (1977)* and the packet-based model due to *Mickley and Fairbanks (1955).*

In summary, the data presented in this paper, complementing the results published previously, provide useful experimental hydrodynamic data for upward flowing dense fluidised particle suspensions, with particular reference to the dimensions of the tubes proposed for use at the focus of a concentrated solar power plant.

Acknowledgements

This work was developed in the frame of the CSP2 Project - Concentrated Solar Power in Particles. This project has received funding from the European Union's Seventh Programme for research, technological development and demonstration under grant agreement N° 282 932. The authors would like to thank Mr Eric Worpe (Department of Electrical and Electronic Engineering, University of Surrey) for his kind assistance in the design and manufacturing of the heat transfer probe.

5. Literature Cited.

1. *Flamant D., Gauthier D., Benoit H., Sans J.L., Garcia R., Boissiere B., Ansart R. and Hemati M. (2013) "Dense suspension of solid particles as a new heat transfer fluid for concentrated solar thermal plants: On-sun proof of concept", Chemical Engineering Science, Vol. 102, 567-57*
2. *Pacio J., Wetzel Th. (2013) "Assessment of liquid metal technology status and research paths for their use as efficient heat transfer fluids in solar central receiver systems", Solar Energy, Vol. 93, 11-22*
3. *Botterill, J.S.M. "Fluid-bed heat transfer", Academic Press, London, 1975*
4. *Mickley H.S., Fairbanks D.F., (1955) "Mechanism of heat transfer to fluidized beds", AIChE J. 1 (3) 374–384*
5. *Baskakov, A.P. & Berg, B.V. "Heat transfer between a fluidized bed and an immersed cylinder". Journal of Engineering Physics (1966) 10: 434*
6. *Thring, R.H. (1977) "Fluidized bed combustion for the stirling engine", Int. J. Heat Mass Trasfer, Vol. 20, pp. 911-918*
7. *Ozkaynak T.F, Chen J.C. (1980) "Emulsion phase residence time and its use in heat transfer models in fluidized beds". AIChE J., Vol.26, 544-550*
8. *Wong Y. S., Seville J. P. K. (2006), "Single-particle motion and heat transfer in fluidized beds". AIChE Journal, Vol.52: 4099–4109*
9. *Seville, J.P.K., Ingram, A., Fan, X., Parker, D.J., (2009) "Positron emission imaging in chemical engineering". In: Li, Jinghai (Ed.), Advances in Chemical Engineering, Vol. 37. Academic Press, pp. 149–178*
10. *Perez Lopez I, Benoit H, Gauthier D, Sans J-L, Guillot E, Mazza G, Flamant G. (2016) "On-sun operation of a 150 kWth pilot solar receiver using dense particle suspension as heat transfer fluid". Solar Energy 137, 463-476*

11. *García-Triñanes P., Seville J.P.K., Boissière B., Ansart R., Leadbeater T.W., Parker D.J. (2016) "Hydrodynamics and particle motion in upward flowing dense particle suspensions: Application in solar receivers" Chemical Engineering Science, 146, 346-356*
12. *Boissiere B., Ansart R., Gauthier D., Flamant G., Hemati M. (2015) "Experimental hydrodynamic study of gas-particle dense suspension upward flow for application as new heat transfer and storage fluid". Canadian Journal of Chemical Engineering, 93 (2), pp. 317-330.*
13. *Ganzha, V. L. and Saxena, S. C. (1998) "Heat-transfer characteristics of magnetofluidized beds of pure and admixtures of magnetic and nonmagnetic particles". International Journal of Heat and Mass Transfer 41,209-218*
14. *Ansart R., García-Triñanes P., Boissière B., Benoit H., Seville J., Simonin O. (2017) "Dense gas-particle suspension upward flow used as heat transfer fluid in solar receiver: PEPT experiments and 3D numerical simulations" Powder Technology, vol. 307, 25-36*
15. **Davidson J.F., Harrison D., *Fluidized Particles*, Cambridge University Press, 1963**
16. *Stein M, Ding Y L, Seville J P K and Parker D J (2000) "Solids Motion in Bubbling Gas Fluidized Beds", Chem. Eng. Sci. 55, 5291-5300*
17. *García-Triñanes P., Seville, J., Ansart, R., Simonin, O., Benoit, H., (2016) "Flow Patterns in High Density Fluidized Beds Used As Solar Energy Carrier Systems". 2016 AIChE Annual Meeting*
18. *Ziegler E. N., Koppel L. B., Brazelton W. T. (1964) "Effects of Solid Thermal Properties on Heat Transfer to Gas Fluidized Beds", Industrial & Engineering Chemistry Fundamentals, 3 (4), 324-328*
19. *Kong W, Tan T., Baeyens J., Flamant G., Zhang H. (2017) "Bubbling and Slugging of Geldart Group A Powders in Small Diameter Columns", Ind. Eng. Chem. Res. 2017, 56, 4136−4144*
20. *Zabrodsky S.S., (1966) "Hydrodynamics and Heat Transfer in Fluidized Beds". Cambridge, MA: MIT Press*

Highlights

- Particle trajectories are determined within a dense upward-moving fluidised bed.

- Particle-to-wall heat transfer coefficients have been measured experimentally.

-Heat transfer coefficients are in the range 180-320 W/m^2K.

-Particle residence times at the wall were found to be distributed according to a log-normal distribution.

-Experimentally-obtained heat transfer coefficients were found to be in good agreement with prior predictions.

Preprint submitted to CES: 20th July 2017
Reviewed 31st October 2017